Electronic Supplementary Material (ESI) for RSC Advances.
This journal is © The Royal Society of Chemistry 2020

Electronic Supplementary Information

Synthesis of size-controlled and highly monodispersed silica nanoparticles using a short alkyl-chain fluorinated surfactant

Saravanan Nagappan,[a] Anandhu Mohan,[a] Anju Maria Thomas,[a] Jong-Man Yoo,[a] Nadim Eid,[b] Ildoo Chung,[a] Bruno Ameduri[b] and Chang-Sik Ha*[a]

[a]Department of Polymer Science and Engineering, Pusan National University, Busan, 46241 Republic of Korea.

[b]Institut Charles Gerhardt, CNRS, University of Montpellier, ENSCM, Montpellier, France.

*corresponding authors: csha@pnu.edu

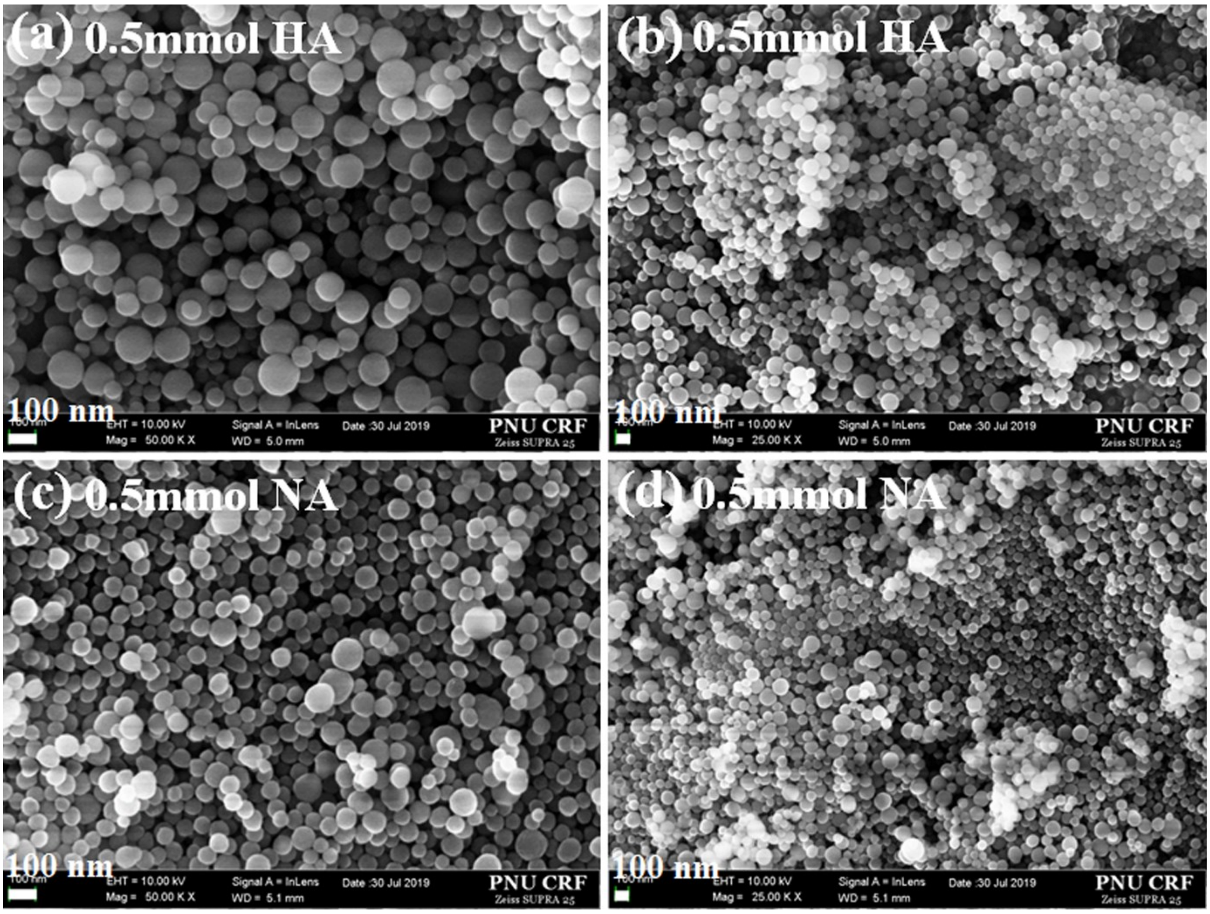

Fig. S1 FESEM images of the SiNPs prepared in the presence of (a and b) HA (0.5 mmol) and (c and d) NA (0.5 mmol) (before calcination, BC).

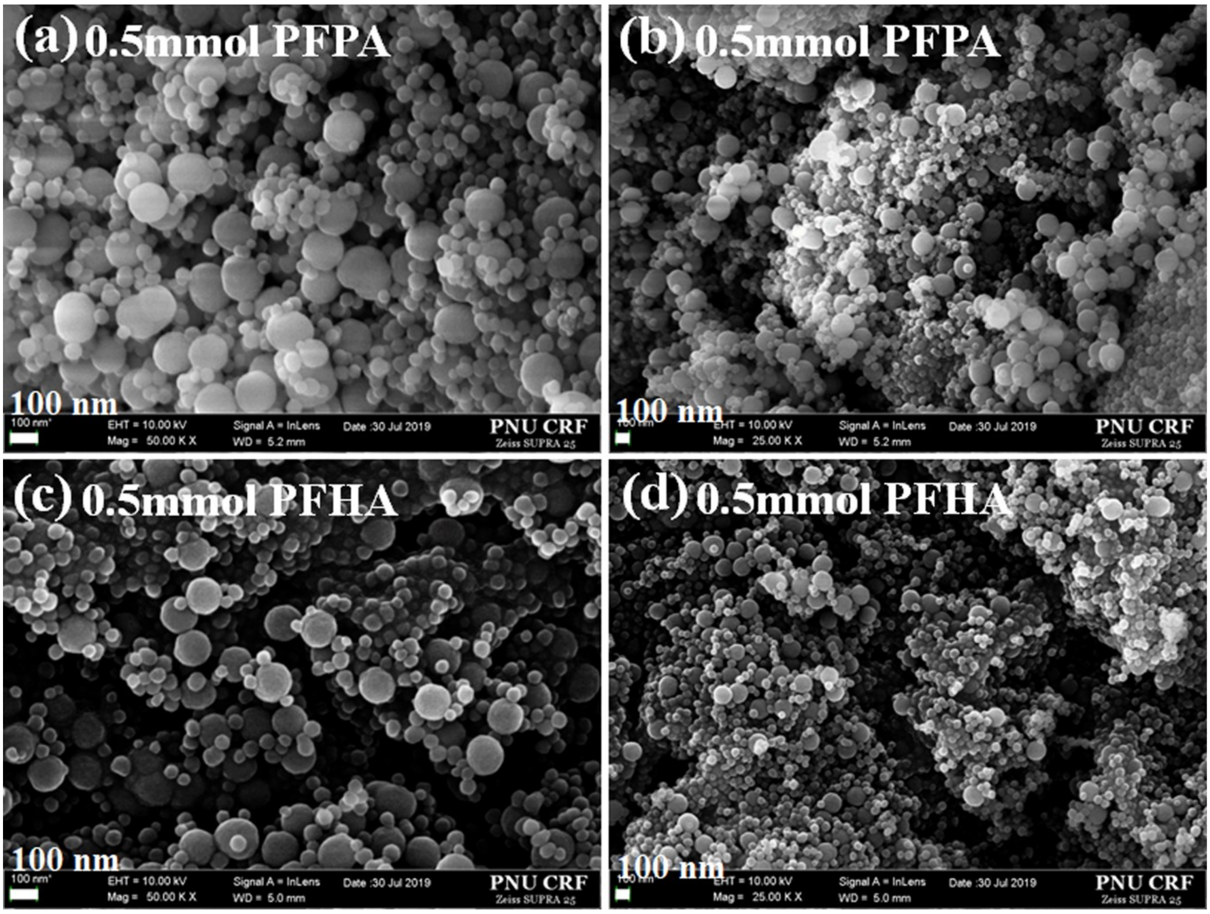

Fig. S2 FESEM images of the SiNPs prepared in the presence of (a and b) perfluoropentanoic acid (PFPA, 0.5 mmol) and (c and d) perfluorohexanoic acid (PFHA, 0.5 mmol), BC.

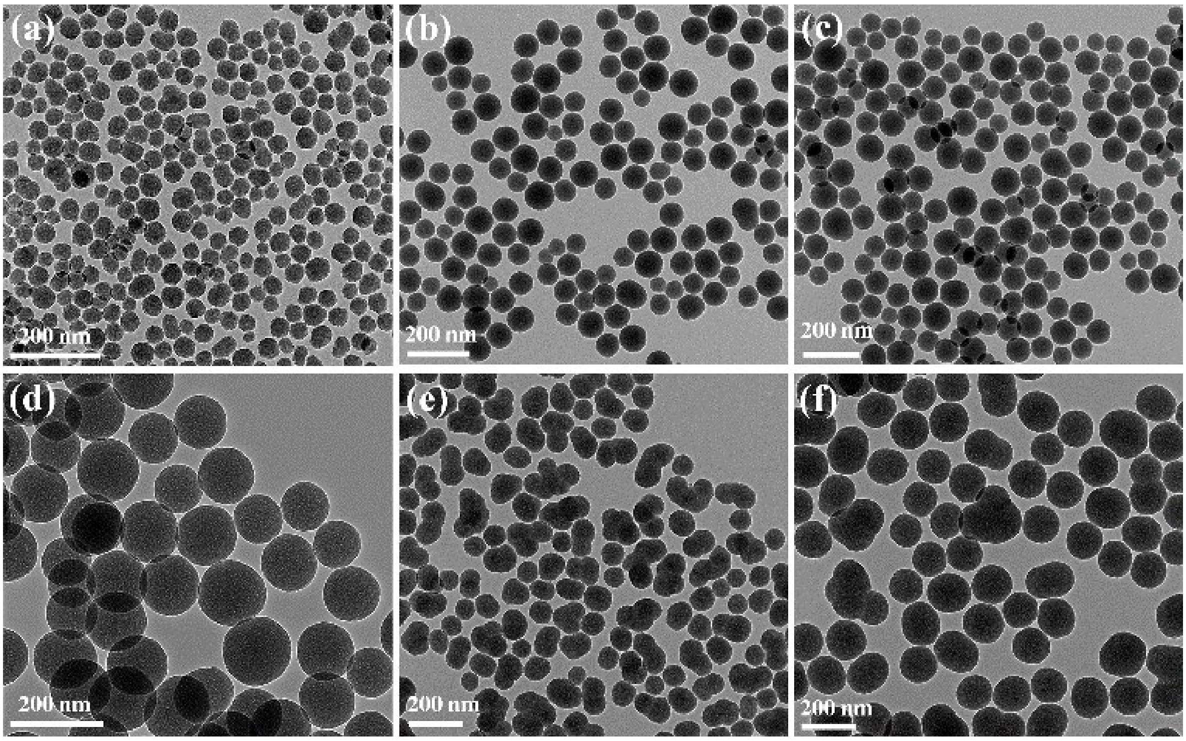

Fig. S3 FETEM images of the SiNPs prepared at lower magnification (a) in the absence of MAF-OH and (b-f) in the presence of MAF-OH at various concentrations, 0.5, 1.0, 1.5, 2.0, and 2.5 mmol, respectively, BC.

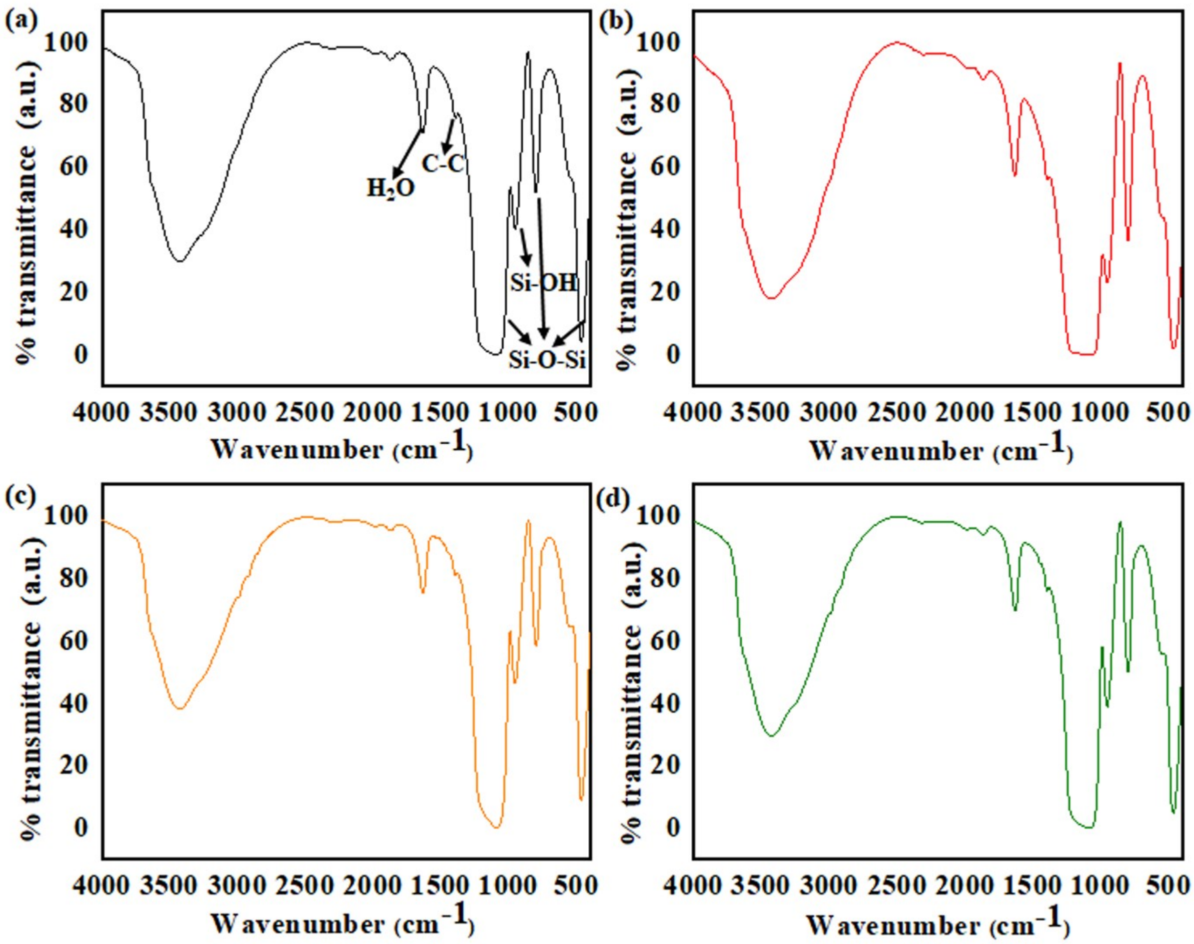

Fig. S4 FTIR spectra of the SiNPs prepared in the presence of 0.5 mmol (a) HA, (b) NA, (c) PFPA, and (d) PFHA surfactants, respectively, BC.

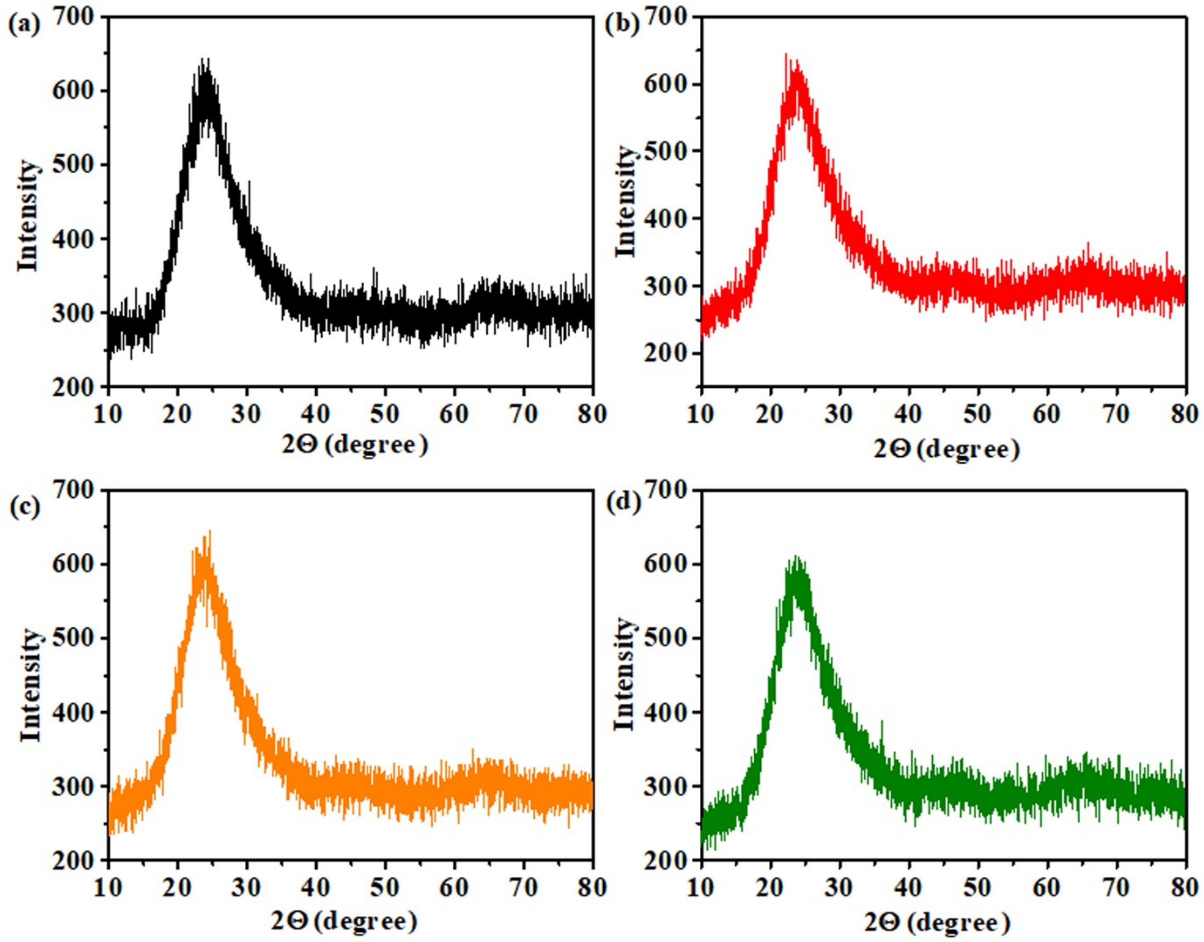

Fig. S5 XRD patterns of the SiNPs prepared in the presence of 0.5 mmol (a) HA, (b) NA, (c) PFPA, and (d) PFHA surfactants, respectively, BC.

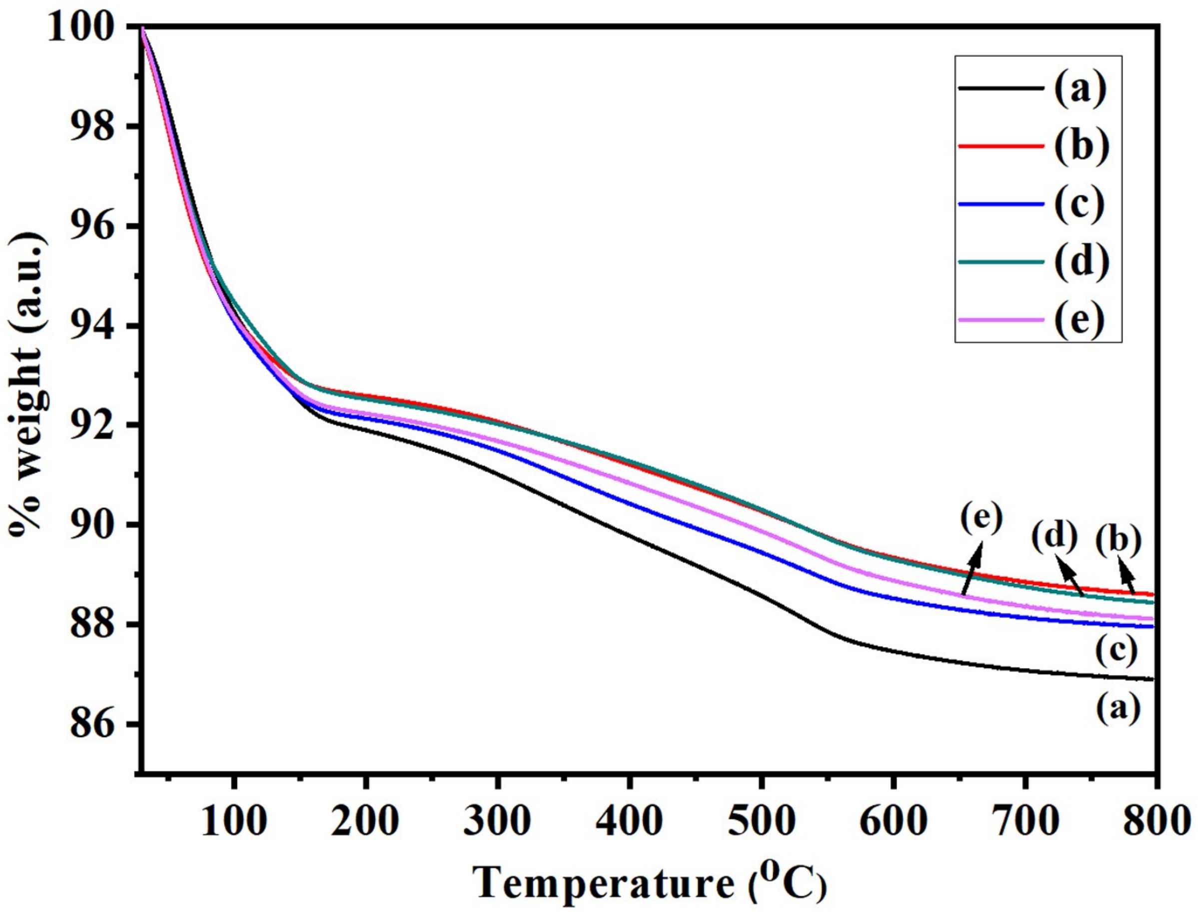

Fig. S6 TGA thermograms (under nitrogen) of the SiNPs prepared in the (a) absence of surfactant, and presence of 0.5 mmol (b) HA, (c) NA, (d) PFPA, and (e) PFHA surfactants, respectively, BC.

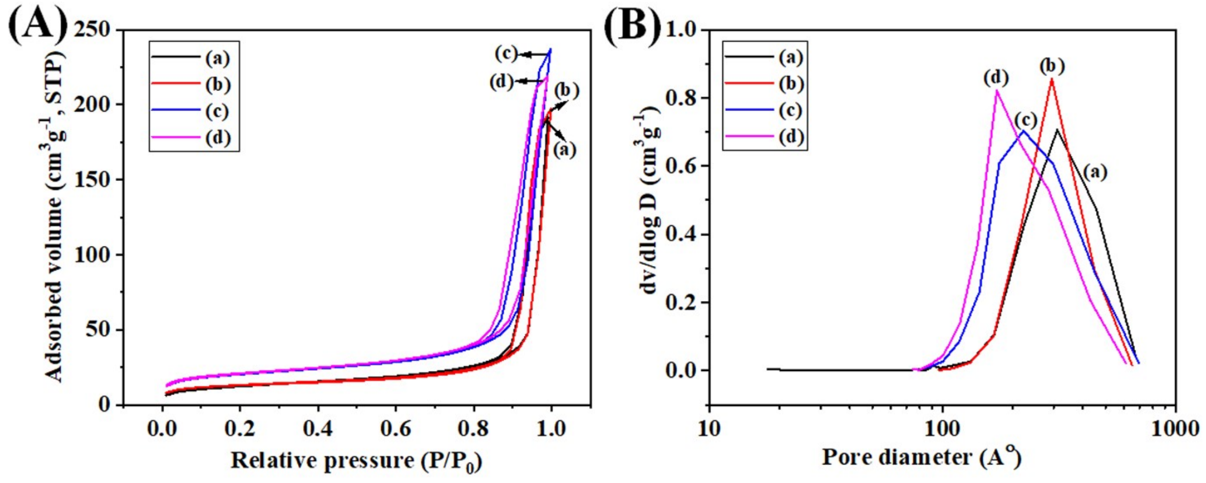

Fig. S7 (A) Nitrogen adsorption and desorption isotherms and (B) pore-size distribution curves of the SiNPs prepared in the presence of 0.5 mmol (a) HA, (b) NA, (c) PFPA, and (d) PFHA surfactants, respectively, BC.

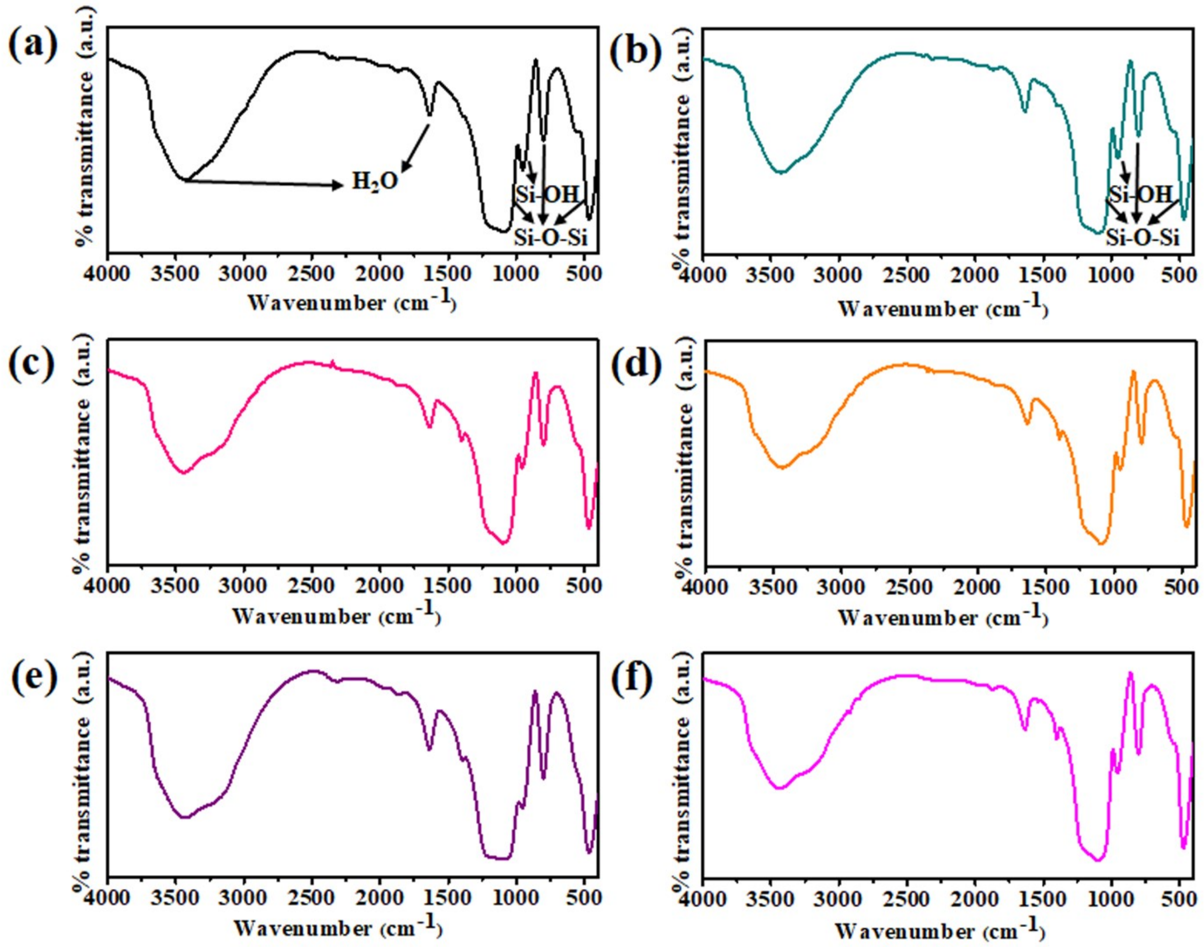

Fig. S8 FTIR spectra of the SiNPs prepared (a) in the absence of MAF-OH and (b-f) in the presence of MAF-OH at various concentrations, 0.5, 1.0, 1.5, 2.0, and 2.5 mmol, respectively, BC.

The FTIR spectrum of the SiNPs prepared in the absence of surfactant exhibits strong transmission peaks at 1080, 800, and 470 cm^{-1}, which indicate asymmetric stretching, symmetric stretching vibration, and rocking vibration peaks of Si-O-Si bonds, respectively (Fig. S8a). The spectrum also illustrates the bending vibration of the Si-OH bond at 950 cm^{-1}.[1] In addition to the above important peaks, the spectrum also depicts the stretching and bending vibrations of the H-OH bond at 3425 and 1638 cm^{-1} due to adsorbed water and the formation of hydroxyl functional groups at the surface (Fig. S8a).[1] A small band at 1400 cm^{-1} appeared due to the increase in the concentration of MAF-OH, suggesting the presence of trace amounts of MAF-OH. Owing to the high solubility of MAF-OH, other peaks did not appear because of the leaching of the surfactant from the sample during the washing cycles (Fig. S8b).[1] This confirms the presence of MAF-OH in the synthesised SiNPs, which is attributed to the formation of highly controlled and uniform SiNPs. Similar FTIR spectra were generated by the increase in the concentration of MAF-OH (Fig. S8c–f). At higher temperatures, MAF-OH can be decomposed by breaking the chemical bonds. This confirmed by the vanishing of the trace peak at 1400 cm^{-1} by the calcination of the samples at 540 °C (Fig. S9). The disappearance of the Si-OH peak at 950 cm^{-1} also suggests the removal of some water molecules by the condensation of hydroxyl groups in the SiNPs. The decrease in the transmission peak at 1638 and 3435 cm^{-1} also illustrates the removal of some water molecules absorbed at the surface.[1] Strong Si-O-Si peaks were observed for all the samples, which indicates that pure SiNPs were developed AC. All other characterisations also proved that MAF-OH plays a significant role in controlling the particle shape, size, and morphology, compared with those observed in SiNPs created without MAF-OH or by using various other surfactants (Figs. S10-S19, and Table S1).

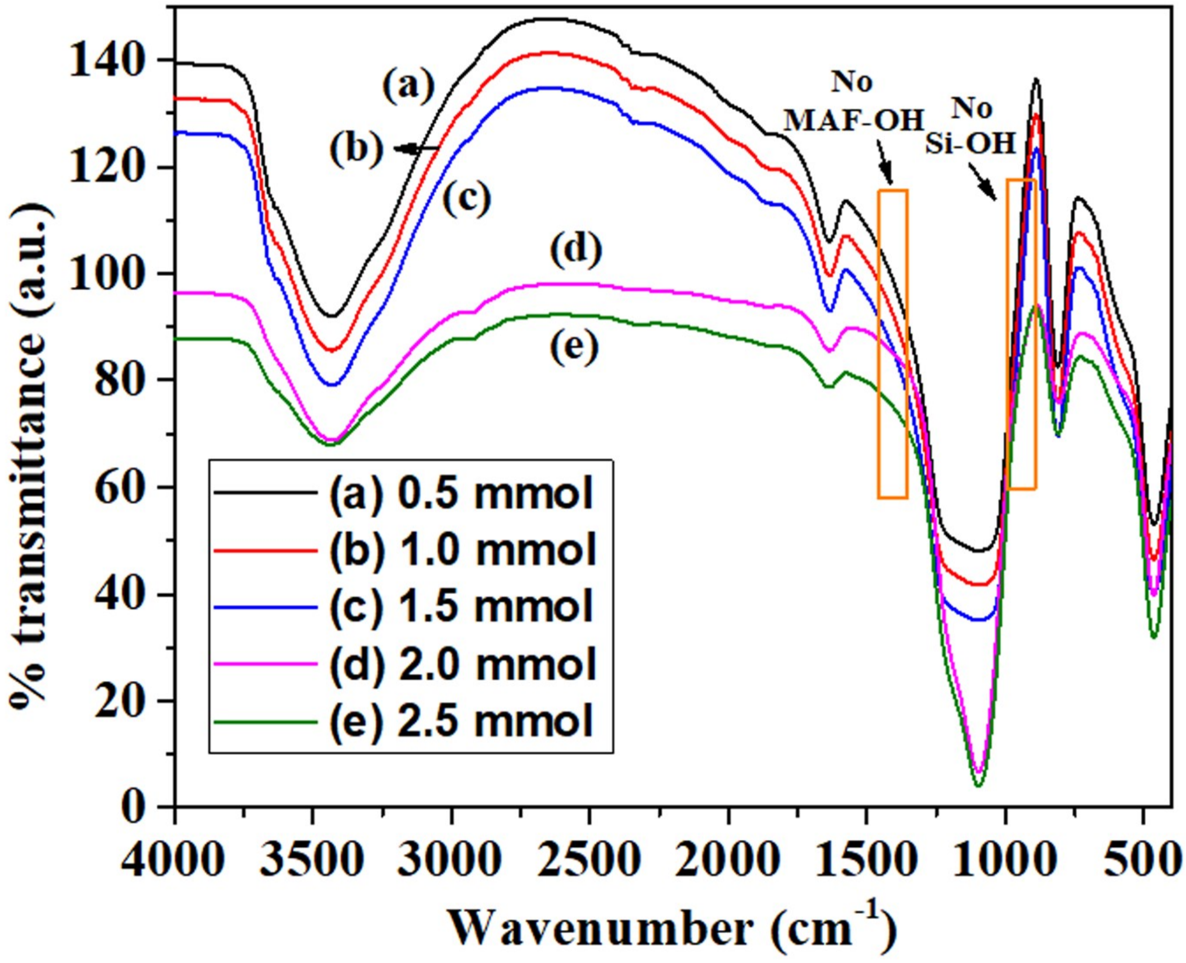

Fig. S9 FTIR spectra of the SiNPs prepared (a-e) in the presence of MAF-OH at various concentrations, 0.5, 1.0, 1.5, 2.0, and 2.5 mmol, respectively, AC.

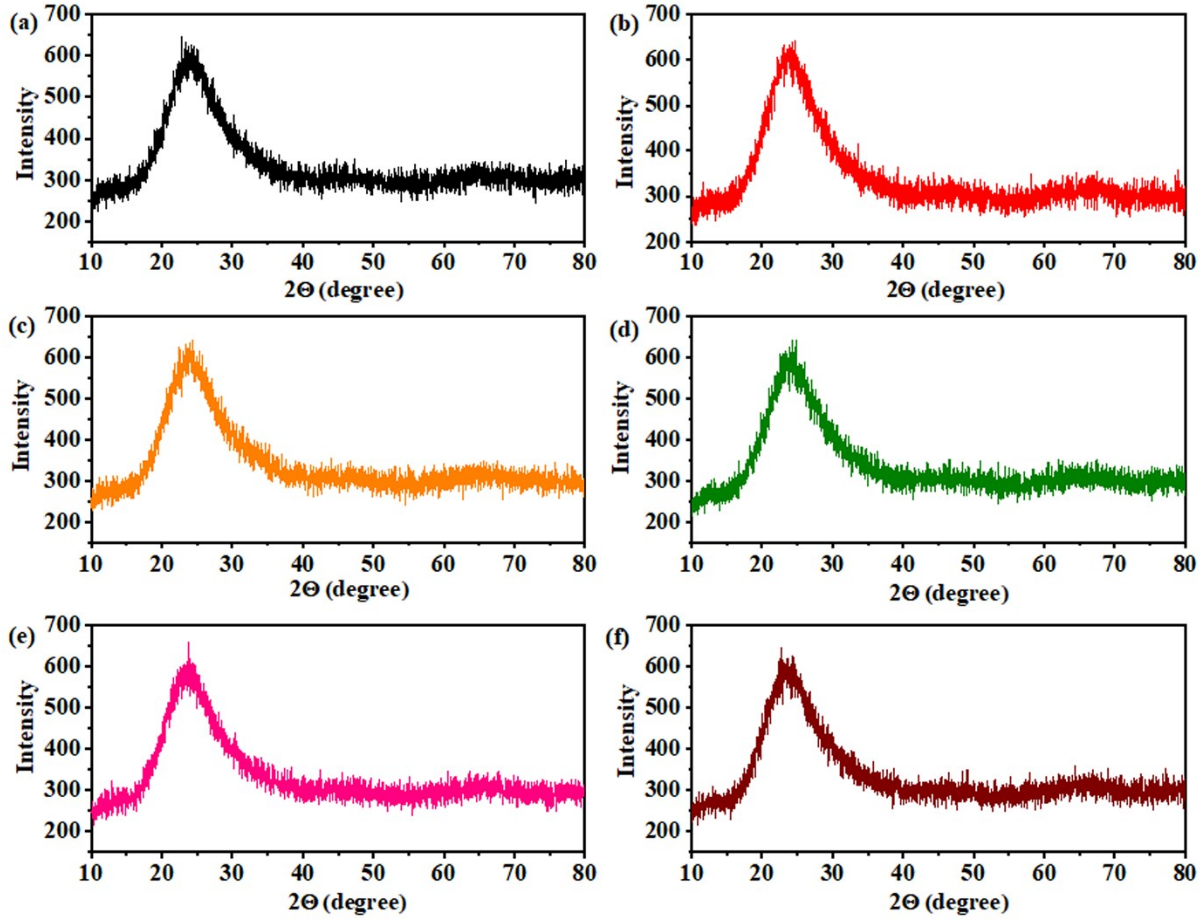

Fig. S10 XRD patterns of the SiNPs prepared (a) in the absence of MAF-OH, (b-f) in the presence of MAF-OH at various concentrations, 0.5, 1.0, 1.5, 2.0, and 2.5 mmol, respectively, BC.

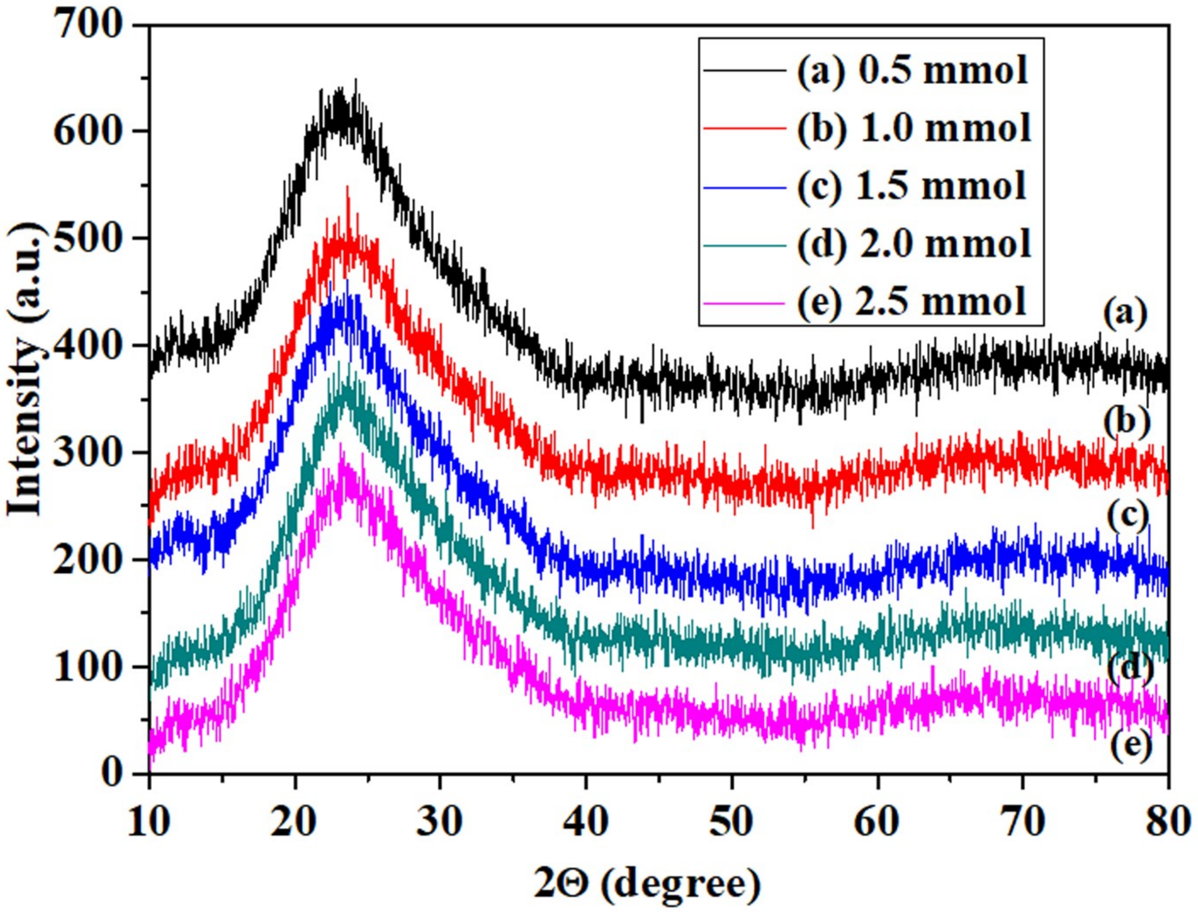

Fig. S11 XRD patterns of the SiNPs prepared (a-e) in the presence of MAF-OH at various concentrations, 0.5, 1.0, 1.5, 2.0, and 2.5 mmol, respectively, AC.

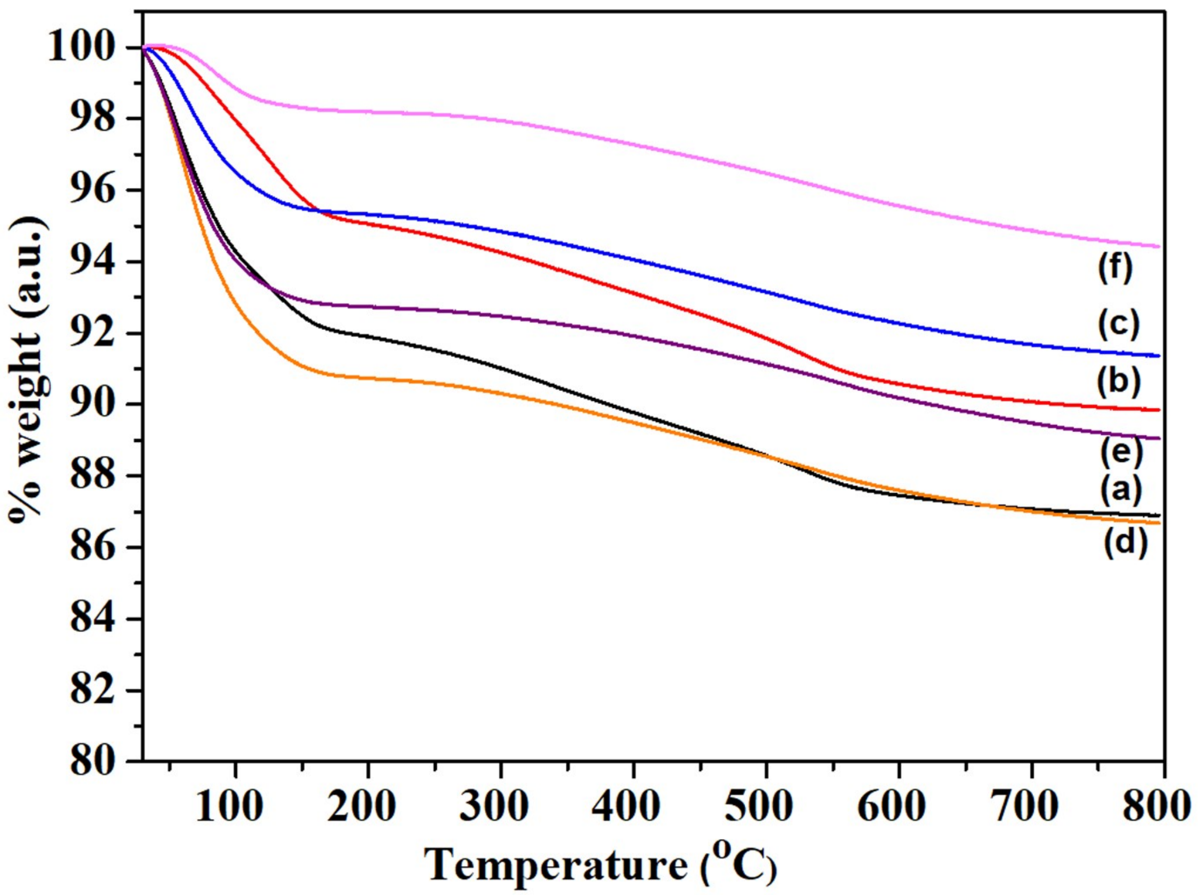

Fig. S12 TGA thermograms of the SiNPs prepared (a) in the absence of MAF-OH, (b-f) in the presence of MAF-OH at various concentrations 0.5, 1.0, 1.5, 2.0, and 2.5 mmol, respectively, BC under nitrogen atmosphere.

Degradation behaviour of MAF-OH and other surfactants

MAF-OH easily flows at a temperature above room temperature. Mostly, the decarboxylation occurs in the MAF-OH from 150 °C, followed by breaking of the fluorinated chains at temperatures above 200-300 °C, and the compound is almost degraded above to more elevated temperature. The degradable behavior of MAF-OH surfactant was reported,[3] releasing F^- ions in pressurized hot water (PHW) by the decomposition of CF_3 group in MAF-OH. More detailed degradation mechanism of MAF-OH can be found in the reference.[3] Similar degradations can be possible for hydrocarbon and some fluorinated surfactants.[4-6] Hori *et al.* reported the decomposition of fluorinated surfactants such as C_5-C_9 perfluorocarboxylic acids (PFCAs) at 80 °C and perfluoroether carboxylic acids at 150 °C with or without persulfate ($S_2O_8^{2-}$) under pressurized air in a sealed reactor.[4] The obtained results suggest that some decomposition occurred for PFHA and traces of decomposition detected for PFPA in the presence and the absence of $S_2O_8^{2-}$ at the temperatures over 300 °C.[5,6] At basic conditions, the fluorinated groups are quite stable. Thus, it can be considered that the material can maintain the structural integrity at basic conditions. Moreover, to the best of our knowledge, MAF-OH would not be degraded under basic pH conditions.

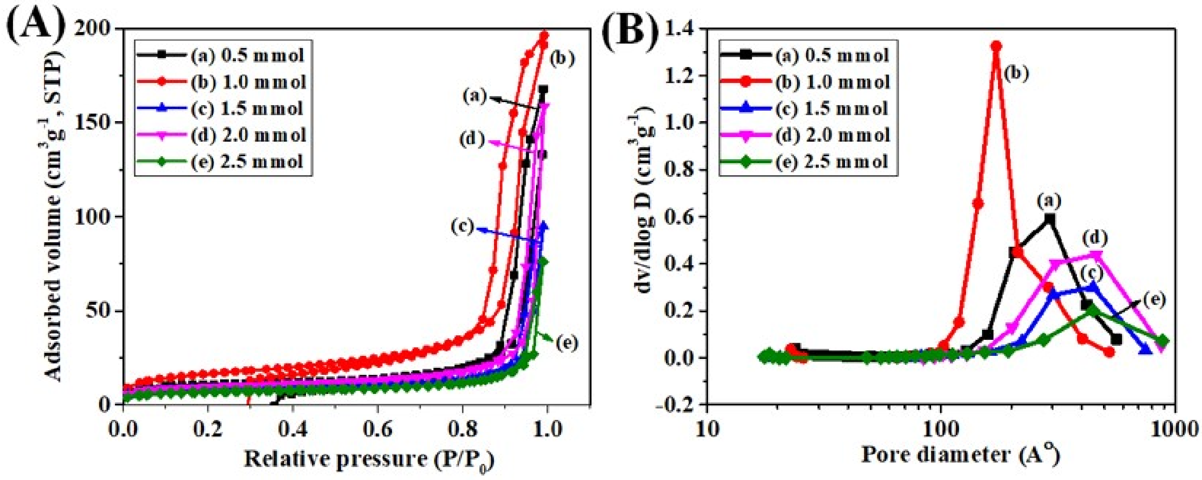

Fig. S13 (A) Nitrogen adsorption and desorption isotherms and (B) pore-size distribution curves of the SiNPs prepared in the presence of MAF-OH at various concentrations, 0.5, 1.0, 1.5, 2.0, and 2.5 mmol (a-e), respectively, AC.

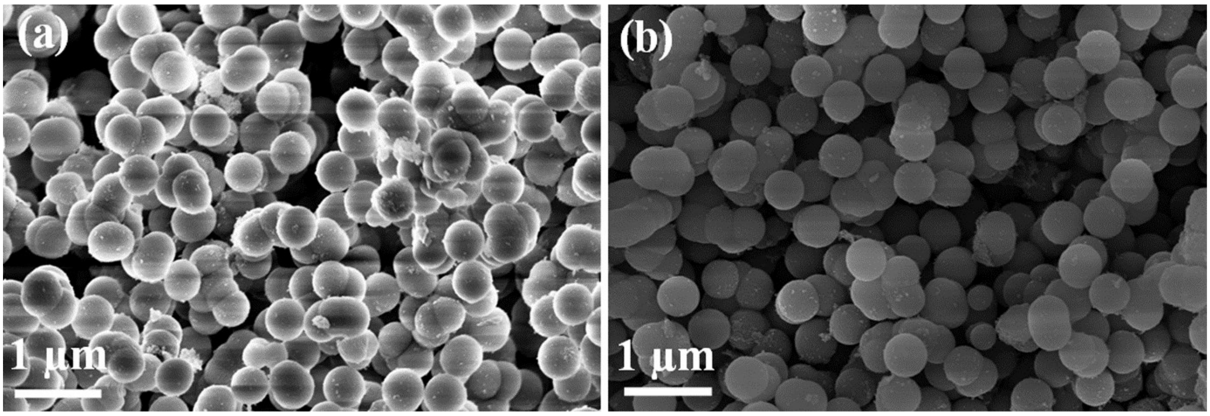

Fig. S14 FESEM images of the SiNPs prepared in the presence of CTAB (a) BC and (b) AC.

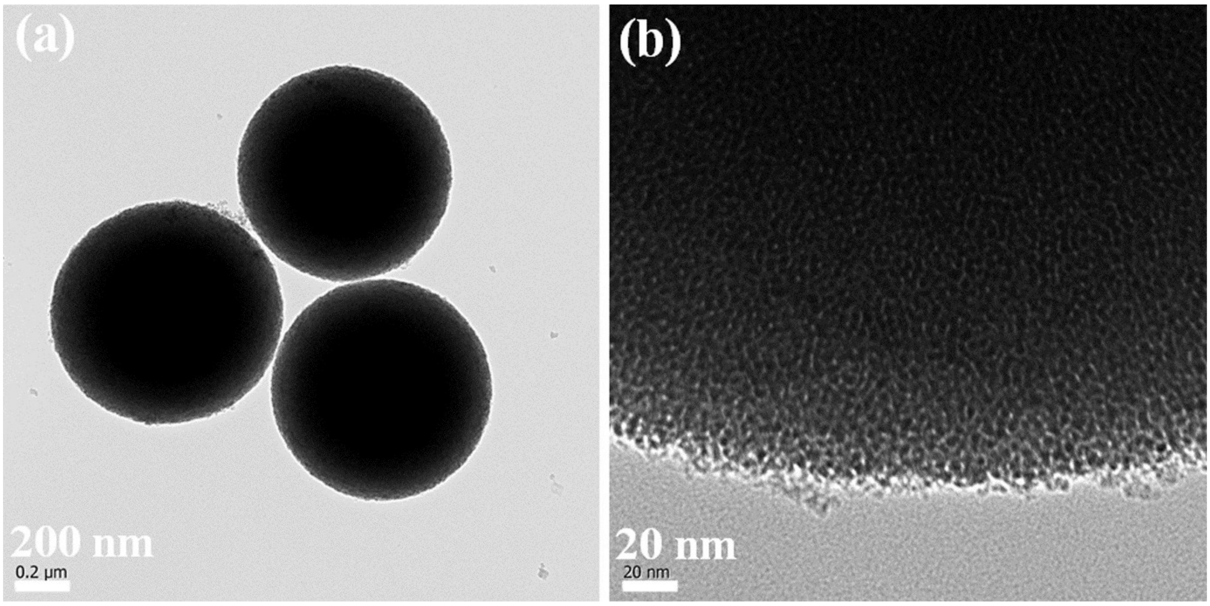

Fig. S15 Lower and higher magnification FETEM images of the SiNPs prepared (a and b) in the presence of CTAB BC.

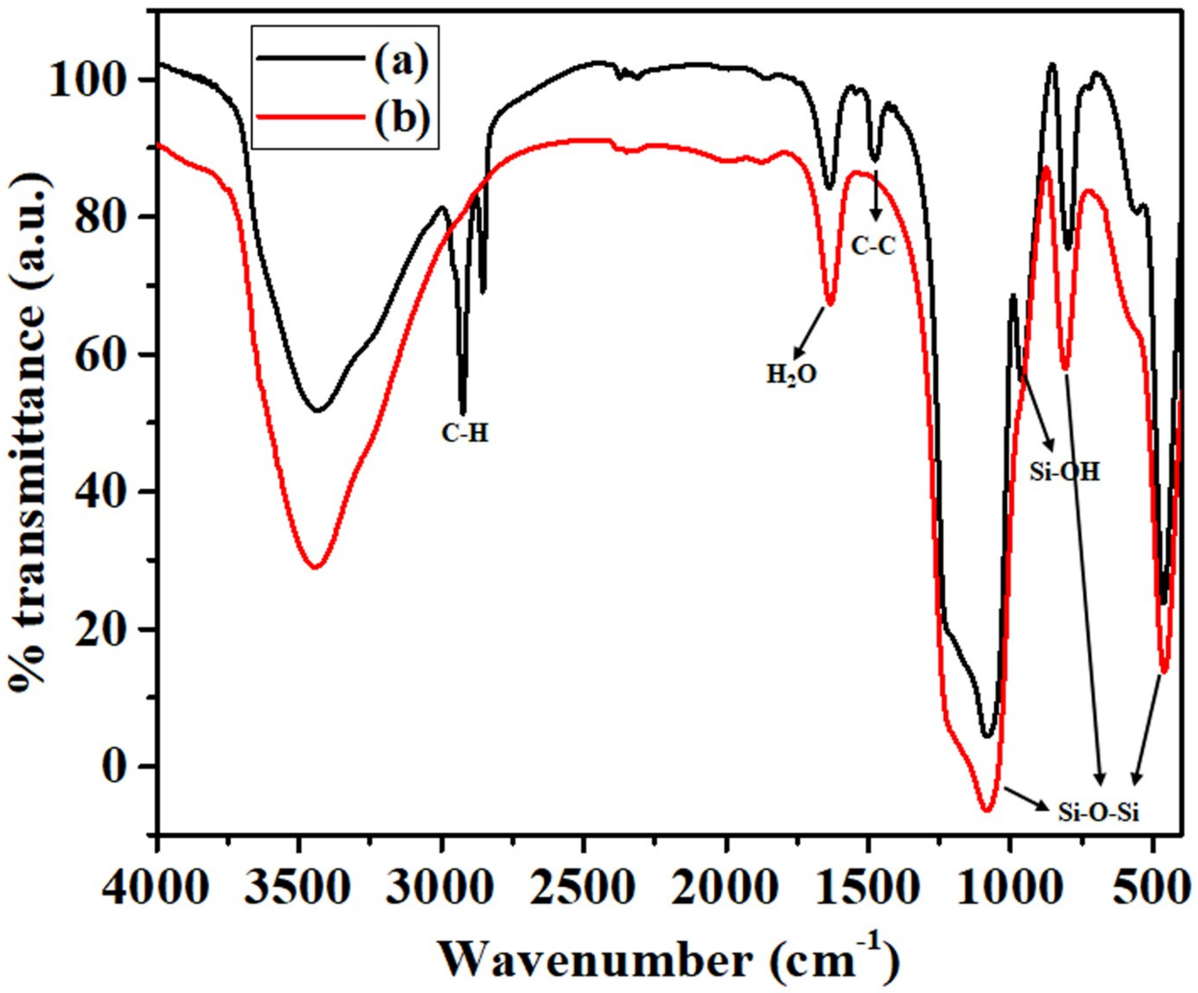

Fig. S16 FTIR spectra of the SiNPs prepared in the presence of CTAB (a) BC and (b) AC.

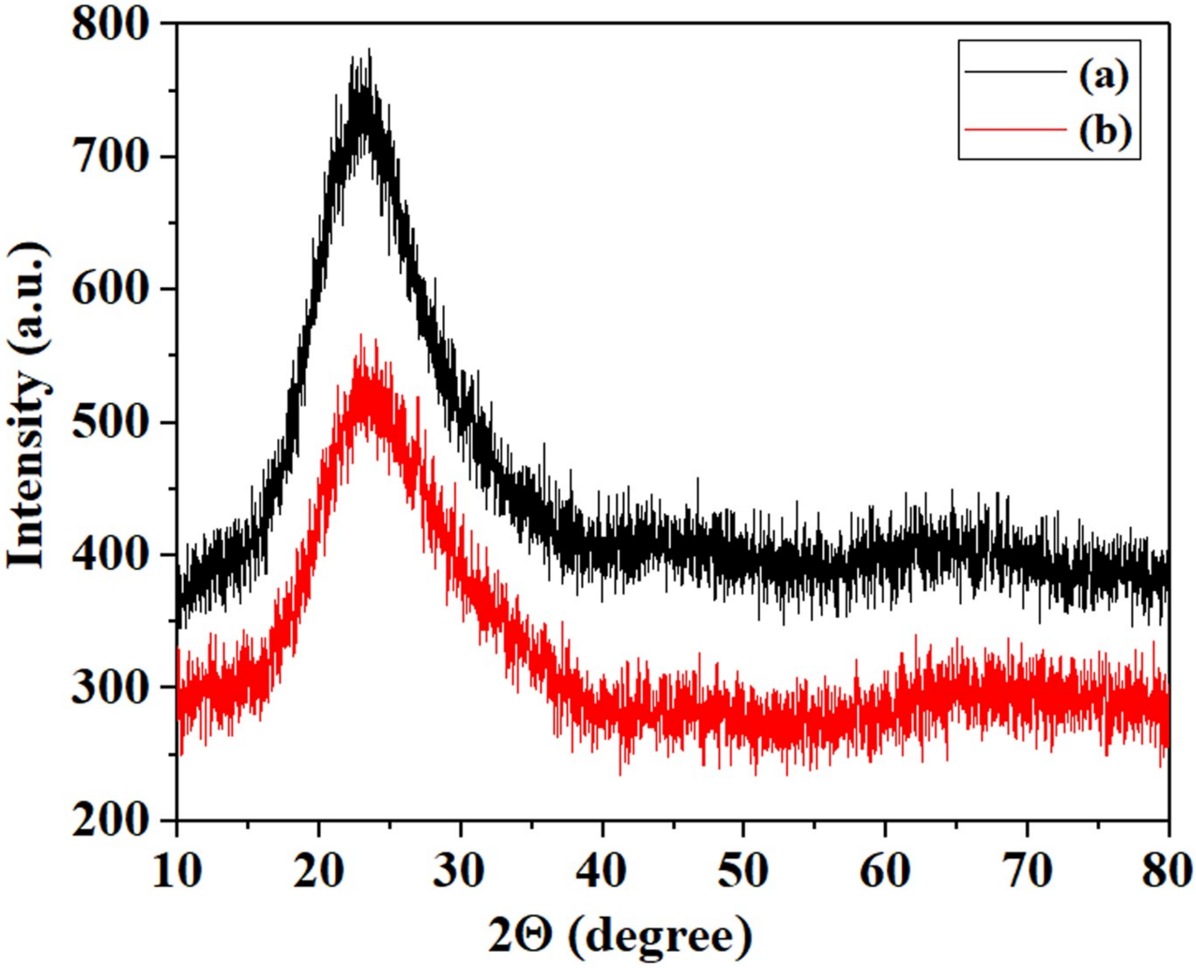

Fig. S17 XRD patterns of the SiNPs prepared in the presence of CTAB (a) BC and (b) AC.

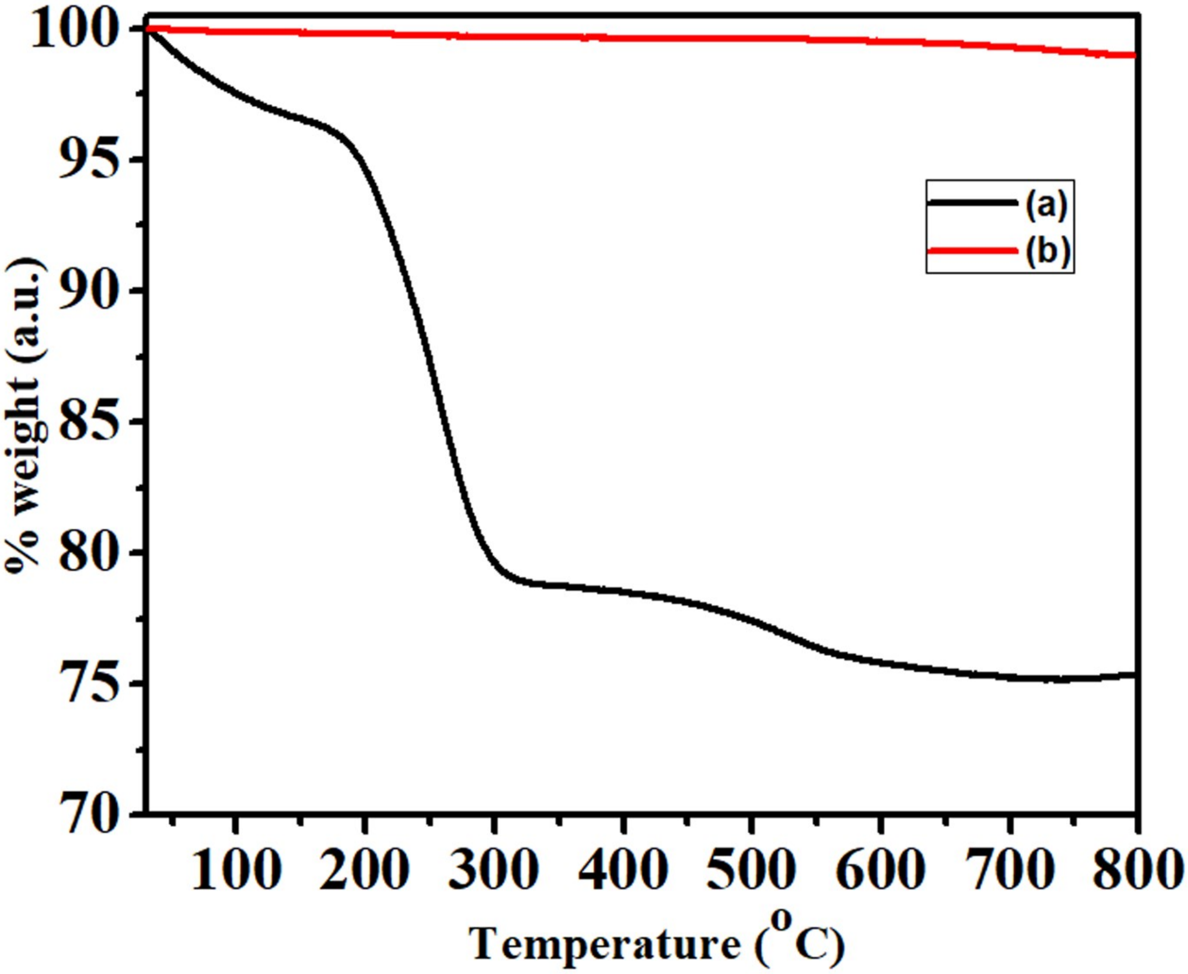

Fig. S18 TGA thermograms of the SiNPs prepared in the presence of CTAB (a) BC and (b) AC.

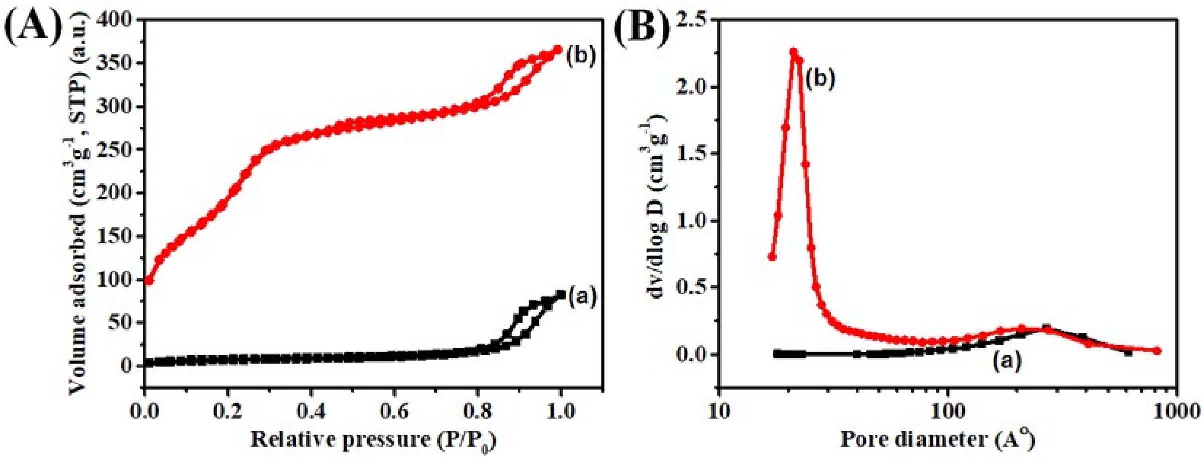

Fig. S19 (A) Nitrogen adsorption and desorption isotherms and (B) pore-size distribution curves of the SiNPs prepared in the presence of CTAB (a) BC and (b) AC.

Table S1 The surface areas, pore volumes, and pore diameters of the samples obtained from the nitrogen adsorption and desorption isotherms and pore-size distribution curves, zeta potential, and average particle size values of samples prepared in the presence of various surfactants, BC and AC.

Sample	BET surface area ($m^2\,g^{-1}$)	Total pore volume ($cm^3\,g^{-1}$)	BJH pore diameter (nm)	Zeta Potential Value (mV)	Average particle Size (nm)
0.5HA (BC)	44	0.30	26.8	-37.9	105 ± 40
0.5NA (BC)	45	0.31	27.3	-10.9	81 ± 20
0.5PFPA (BC)	69	0.37	21.2	-37.6	53 ± 12 131 ± 8
0.5PFHA (BC)	70	0.34	19.3	-14.4	58 ± 8 156 ± 15
0.5CTAB (BC)	26	0.13	27.0	-33.6	760 ± 40
0.5CTAB (AC)	831	0.57	2.2	-6.2	777 ± 40

Note: Here, we mentioned two average particle size values for 0.5PFPA (BC) and 0.5PFHA (BC), because these samples have dual particle sizes (Fig. S2), and these average particle sizes cannot be compared with each other. Thus, we provided both values separately in Table S1.

Notes and references

1 K. L. Feng Yan, Jianguo Jiang, Xuejing Chen, Sicong Tian, *Ind. Eng. Chem. Res.*, 2014, **53**, 11884−11890.

2 H. C. Clark and W. S. Tsang, *J. Am. Chem. Soc.*, 1967, **3**, 533–539.

3 S. Banerjee, J. Schmidt, Y. Talmon, H. Hori, T. Asai and B. Ameduri, *Chem. Commun.*, 2018, **54**, 11399–11402.

4 H. Hori, Y. Nagaoka, M. Murayama and S. Kutsuna, *Environ. Sci. Technol.*, 2008, **42**, 7438–7443.

5 S. Wang, Q. Yang, F. Chen, J. Sun, K. Luo, F. Yao, X. Wang, D. Wang, X. Li and G. Zeng, *Chem. Eng. J.*, 2017, **328**, 927–942.

6 F. Xiao, P. C. Sasi, B. Yao, A. Kubátová, S. A. Golovko, M. Y. Golovko and D. Soli, *Environ. Sci. Technol. Lett.*, 2020, **7**, 343−350.